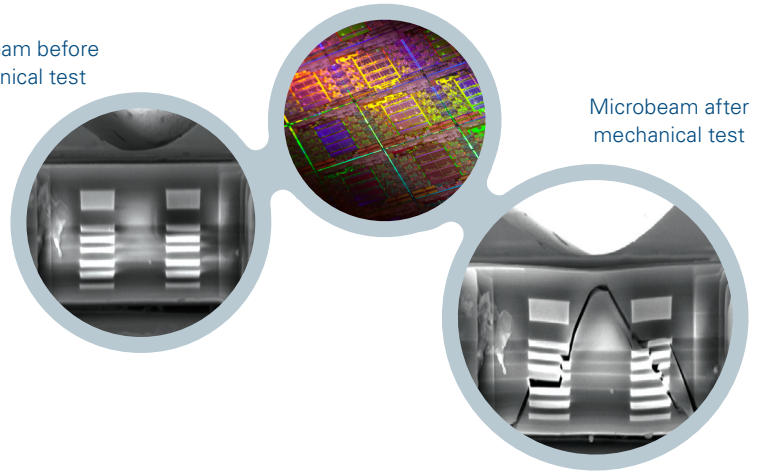


Microbeam before
mechanical test



Microbeam after
mechanical test

Application Note #1501

In-Situ Mechanical Testing of Semiconductor Devices

As advancements are made in the performance of semiconductor devices, changes in materials and processing techniques are often required. The trend towards miniaturizing these devices inherently involves components at or approaching the nanoscale. The mechanical properties of materials at this scale can be vastly different from bulk material, which introduces new concerns both during processing and in field use. A reliable testing technique is critical for evaluating the structural stability of these devices. This application note discusses the use of a Hysitron® PI 85L SEM PicoIndenter® is used to investigate the failure mechanisms involved in FIB-milled back-end-of-line (BEOL) microbeam samples.

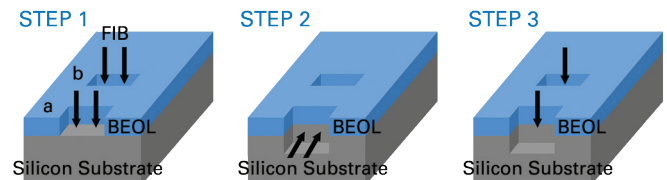


Figure 2. Schematic of sample preparation using FIB-milling.

BEOL Microbeam Sample Preparation

In the microelectronics industry, the properties of individual device components (such as thin films on Si wafers) are often studied to assess their suitability for use in devices. While this can be a useful first step, it is an inadequate representation of the true behavior of those components once incorporated into full structures. In-situ testing not only allows for the evaluation of complete interconnect stacks, the failure mechanisms can also be observed directly with an electron microscope. In this study, the BEOL structures containing seven metal layers were studied in-situ.

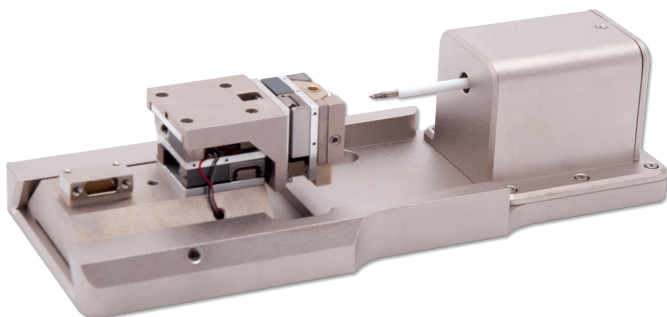


Figure 1. Hysitron PI 85L SEM PicoIndenter.

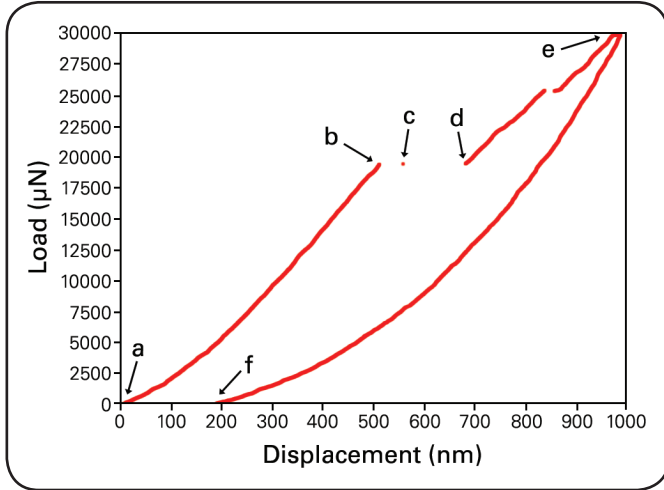
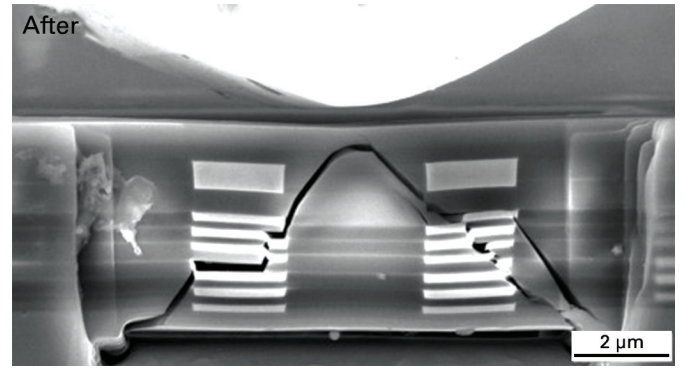
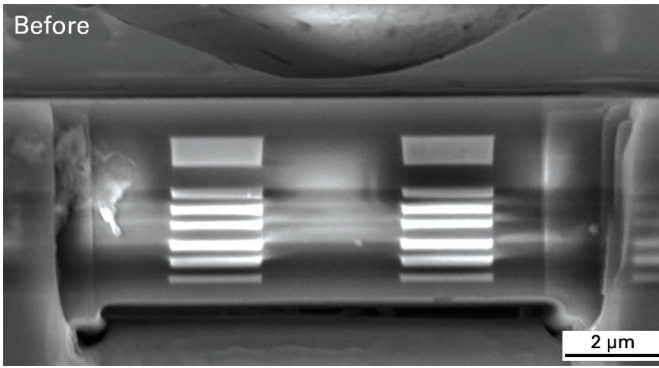


Figure 3. Beam 1 before and after mechanical testing, and the corresponding load vs. displacement curve. Interfacial delamination is observed between the Cu layers and the brittle dielectric.

In order to test these samples in the SEM, three-point microbeam samples were prepared using a focused ion beam (FIB) system, as shown in Figure 2. The microbeams were milled from the cleaved edge of the BEOL sample using a three-step milling process to minimize ion implantation.

The sample was first milled top-down, defining the beam length and coarse width. The beam was then released from the underlying substrate by tilting the sample 90° and undercutting the sample until the material underneath the beam was removed. Finally, the sample was milled top-down a second time, defining the final width of the beam. Four beams with two different lengths and two different widths were prepared, as summarized in Table 1. The specific geometry of these samples also lends itself particularly well to finite element modeling (FEM).

Beam	Length (μm)	Width (μm)	Thickness (μm)	Loading Rate (μN/s)	Critical Load (mN)	Critical Displacement (mN)
1	9.7	4.4	4.3	750	19.4	513
2	19.1	4.4	4.3	500	9.7	9.8
3	9.6	2.0	4.1	500	9.0	534
4	19.1	2.0	4.4	200	4.6	540

Table 1: Summary of the dimensions, loading rates, and critical loads and displacements for each beam. As expected, for beams of a fixed length, the critical load is linearly dependent on width. Similarly, for beams of a fixed width the critical load is inversely proportional to length.

In-Situ Testing

The sample (containing all four beams) was mounted on an instrument-compatible microscopy stub using conductive adhesive, and mechanically secured in the Hysitron PI 85L. In the SEM the beams were tested in load-controlled mode using a wedge-shaped conductive-diamond tip. Applied loading rates ranged from 200 to 750 $\mu\text{N/s}$ (see Table 1), and video was acquired during each test for synchronization to the recorded mechanical data.

The load-displacement curve and corresponding scanning electron micrographs for Beam 1 are shown in Figure 3. In the region of the curve marked a**→**b, the beam is bending. As a critical force is reached (b and c), this is followed by crack initiation and growth in a cohesive and adhesive manner toward the edge of the beam (d**→**e), and then unloading (e**→**f). This type of fracture pattern was observed in beams 1, 2, and 3. However, for beam 4 (shown in Figure 4) a different failure mechanism was observed—a single crack opened at the bottom of the beam, opposite the point of loading.

Finite Element Modeling

The uniform geometries of the microbeam samples are particularly well suited to complementary finite element modeling of the bending tests. A 2D FEM analysis of beam 4 was performed, which clearly supports fracture initiation from locations with highest values of maximum principal stress. In contrast, the fracture patterns in beams 1-3 were found to correlate best to von Mises stress distribution. This suggests two distinct and competing fracture mechanisms, one which is driven only by normal stresses and the other which is driven by shear stress. The prevailing mechanism is thought to be determined by a number of different parameters, including the distribution of copper within the brittle dielectric (which dictates the ability to follow a brittle or ductile fracture pattern), the loading rate, and the specific beam geometry.

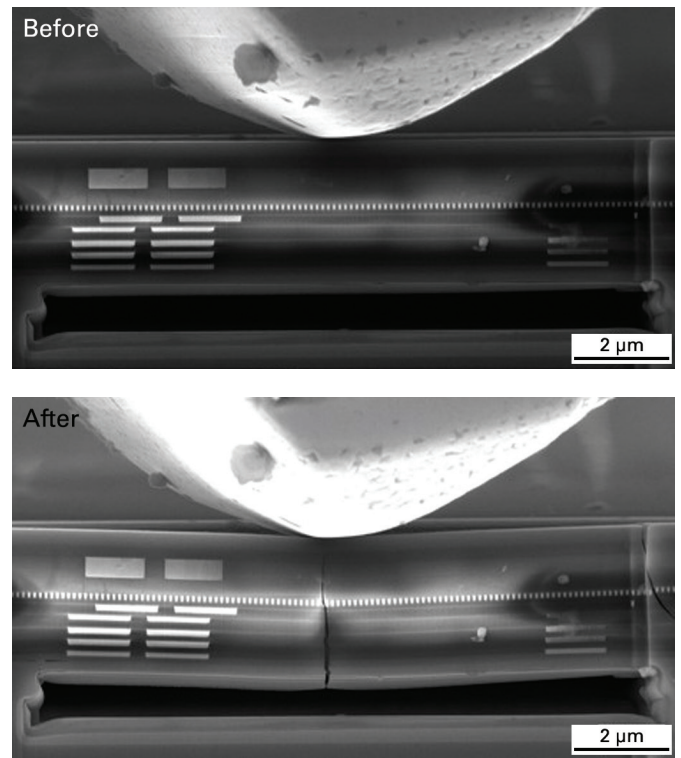


Figure 4. Beam 4 before testing and at critical load. In this beam, a crack opened directly opposite the point of loading.

Conclusions

Quantitative in-situ mechanical testing in the electron microscope allowed for direct observation of cohesive and adhesive crack propagation in FIB-milled beam samples of BEOL structures. The mechanisms responsible for failure in each beam were likely determined by a number of factors, as supported by direct observation in the electron microscope and by FEM analysis.

This in-situ technique can be used to characterize the nature of the failure mechanisms within individual device components, but for complete structures as well; structures with an ever increasing degree of internal complexity. Furthermore, the combination of this experimental technique and modeling makes it possible to identify the weak interfaces in a structure, beyond what can be predicted by the measurement of individual layers. This provides crucial information for device development and manufacturing that had previously been difficult to acquire.

Acknowledgements

Data courtesy of K. Vanstreels, IMEC, Leuven, Belgium.
For more information see Vanstreels, et. al., Appl. Phys. Lett. 105, 213102 (2014).



Bruker Nano Surfaces Division

Minneapolis, MN · USA

+1.952.835.6366

productinfo@bruker.com

www.bruker.com/nanomechanical-testing